EPJ manuscript No.
(will be inserted by the editor)

Principles of Thermoacoustic Energy Harvesting

Andrew W Avent[1] Chris R Bowen[1]

Dept. Mechanical Engineering, University of Bath, Claverton Down, BATH, BA2 7AY

Abstract. Thermoacoustics exploit a temperature gradient to produce powerful acoustic pressure waves. The technology has a key role to play in energy harvesting systems. A time-line in the development of thermoacoustics is presented from its earliest recorded example in glass blowing through to the development of the Sondhauss and Rijke tubes to Stirling engines and pulse-tube cryo-cooling. The review sets the current literature in context, identifies key publications and promising areas of research. The fundamental principles of thermoacoustic phenomena are explained; design challenges and factors influencing efficiency are explored. Thermoacoustic processes involve complex multi-physical coupling and transient, highly non-linear relationships which are computationally expensive to model; appropriate numerical modelling techniques and options for analyses are presented. Potential methods of harvesting the energy in the acoustic waves are also examined.

1 Introduction

Thermoacoustics exploit a temperature gradient to produce powerful acoustic pressure waves. The technology has a key role to play in energy harvesting systems. The field encompasses the thermo-fluid processes associated with the compression and rarefaction of the working gas as an acoustic wave propagates through closely spaced plates in the stack of a thermoacoustic device; and the acoustic network that controls the phasing and properties of the wave.

Send offprint requests to: Dept. Mechanical Engineering, University of Bath, Claverton Down, BATH, BA2 7AY

1.1 A Time-line in the Development of Thermoacoustics

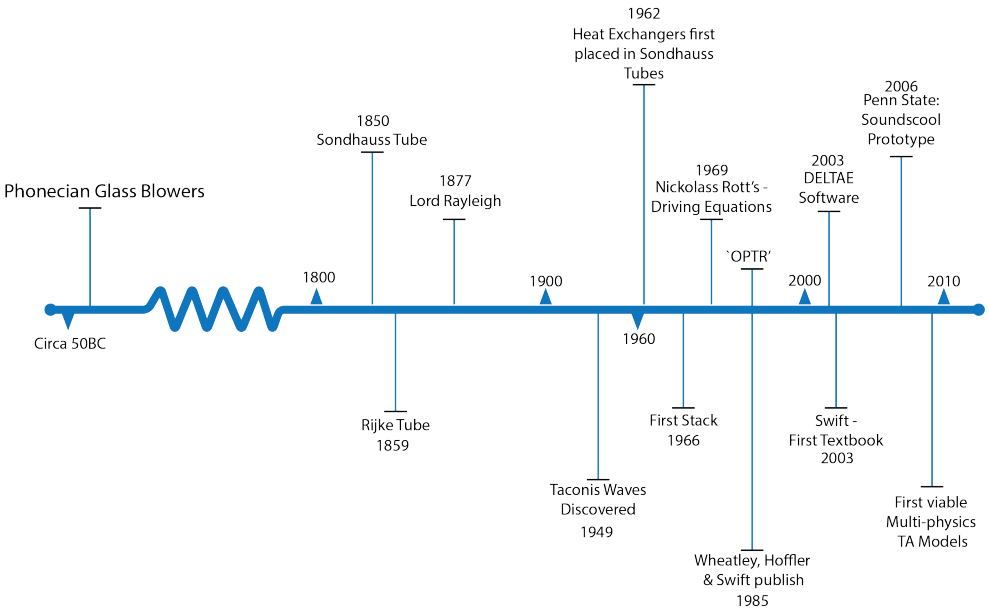

Fig. 1: A time-line in the development of Thermoacoustics.

The time-line in figure 1 summarises the events which have lead to our current understanding of the subject and serves to illustrate the relative youth of the field,in spite of its ancient roots.

50 BC Phoenician Glass blowers, according to Stern and Schlick-Nolte [55] the art of glass blowing (creating glass vessels by inflating molten glass placed on the end of a tube through which the glass worker gently blows) began around 50BC in Lebanon and Israel, in all probability, it was these early glass-blowers who were the first to witness thermoacoustic phenomenon - that of a sound being emitted from the blowpipe when the hot molten glass is attached to it and also from a hot blown glass vessel as it cools.

1850 Carl Sondhauss, according to Feldman et al. [11], was the first to attempt to describe the phenomenon of the sound emission from a hot glass vessel. The Sondhauss tube is effectively a quarter wave thermoacoustic device in which oscillating pressure waves are emitted in response to the application of heat to a closed end glass vessel.

1859 Pieter Rijke Rijke [46] used his Rijke tube to demonstrate thermoacoustic phenomenon, his device comprised a simple vertical glass tube some 0.8m in length and 35mm in diameter with a wire gauze placed approximately 200mm from the bottom end. Heat is applied via a spirit lamp and when the wire gauze glows red the heat source is removed. An oscillating pressure wave, in the form of sound, is emitted from the open top end until the gauze cools.

1877 Lord Rayliegh used a large scale Rijke tube as a lecture demonstration tool - he describes the sound "rising to such intensity as to shake the room". He also gave the first correct explanation of how the sound is generated and in particular the mechanism behind the operation of the Sondhauss Tube in his publication " The Theory of Sound", [45]

1949 Taconis waves discovered described by Bisio and Rubatto [9] as the effect when the end of a gas filled tube is placed in a liquid at cryogenic temperatures emitting a singing sound, similar to Rijke tube, upon its removal and subsequent warming to ambient temperatures.

1962 Heat exchangers were first placed in Sondhauss tubes by Carter White and Steele according to Mortell [30].

1966 Introduction of the stack The first published accounts of porous plugs (stacks) being placed in Sondhauss tubes is by K.T Feldman. These 'stacks' have since been refined as accurately spaced parallel plates through which the acoustic wave passes.

1969 Nickolass Rott first published the governing equations of thermoacoustics following his analysis of Taconis waves and Sondhauss tubes. Modern applications and modelling of thermoacoustics owes much to the work of Rott, [49].

1970 A comprehensive study of heat driven pressure oscillations in a gas was published by Feldman which helped to drive thermoacoustic knowledge forward. [11].

1985 Wheatley, Hoffler and Swift published their research in the American Journal of Physics into thermoacoustic phenomenon and its application to acoustical heat engines [64].

2001/3 G Swift and Garrett published their paper and later the first text book on thermoacoustics in the Journal of the American Acoustical Society - *Thermoacoustics - A unifying perspective for some engines and refrigerators* has become a key reference text in the field and is backed up by a software programme called DeltAE which models thermoacoustic devices, their geometry and architecture. [58].

1.2 Principal Characteristics

Thermoacoustic devices have four particularly interesting characteristics which are of interest in the field of energy harvesting:

(i) The working gasses are generally noble and/or inert.
(ii) The process involves no phase change and therefore is extremely versatile and capable of operating over a wide range of temperatures; in contrast to traditional devices which are governed by the temperatures and pressures associated with the vaporisation and condensation of an 'application specific' working fluid.
(iii) Control systems can be proportional rather than binary (on/off). Binary control has inherent inefficiencies owing to overshoot and tolerance around the ideal temperature (compressors cutting in and out); proportional control allows the device to be run at the correct power output for a given load. [1]
(iv) There are very few moving parts, they are inherently simple and therefore offer the possibility of being both reliable and economic to produce.

2 The Thermoacoustic effect

Thermoacoustics is, as the name implies, a blend of two distinct fields; Thermodynamics and Acoustics. Sound waves, propagating through a compressible working

[1] The control systems associated with a proportional device are inherently more complex but reward us with increased efficiency and an increased temperature range in operation.

fluid and interacting with a stack of closely spaced plates build a local temperature gradient along the plates in the direction of wave propagation. The positional displacement associated with the propagation of the wave, is accompanied by an increase in pressure and temperature (enthalpy) in the wave and a transfer of this heat into the plates which act as a thermal buffer. The subsequent rarefaction of the working fluid results in a decrease in pressure and temperature, at which point the plates transfer heat back into the fluid.

The reciprocating (sinusoidal) displacement of the fluid leads to a temperature gradient along the plates as a result of each fluid element giving up heat during its compression cycle and gaining heat during its rarefaction leading to a 'bucket chain' effect building a temperature gradient along the plates. (see figure 2) The thermal contact and heat transfer between the gas and the plates must be deliberately imperfect. If it were too good, the gas would remain at (or near) the temperature of the adjacent plates; if too poor, there would be insufficient heat transfer for any thermoacoustic effect to take place.

Conversely, a temperature gradient applied across the stack of plates described above will, amplify pressure perturbations to produce a powerful acoustic wave which is, its self, capable of doing work, as in a thermoacoustic engine or prime mover. It is this mode in which the thermoacoustic effect can be used to exploit a temperature gradient in energy harvesting. With reference to figure 7 it can be seen that if, at the point of maximum compression, the gas is further heated as a result of being in close contact with the plate which is at a higher temperature; and if, at the point of maximum rarefaction, the gas is further cooled as a result of being in close contact with the plate which is below the temperature of the gas; an amplification of the acoustic wave results.

The onset temperature gradient (the temperature gradient at which the natural perturbations in the gas are amplified sufficiently to produce an acoustic wave) is illustrated in figure 13 and explained in section 5.4.

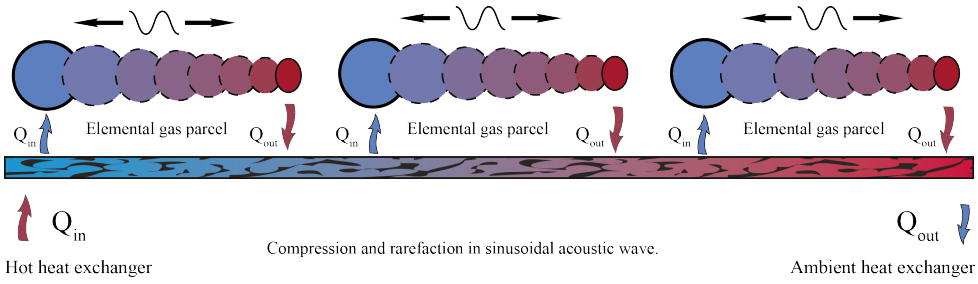

Fig. 2: Temperature gradient built as the result of the bucket-chain effect.

The thermodynamic process which best describes the heat transfer carried out in the regenerator is the 'Stirling' cycle, an idealised analysis is provided below together with a description of the improved Stirling cycle which more closely approximates the true cycle within the regenerator of a thermoacoustic device.

2.1 Idealised Stirling Cycle Analysis

Figure 3 provides a simplified ideal Stirling cycle analysis using a pressure vs volume (PV) diagram, each stage is then related to the simple Stirling cycle schematic shown in figure 4.

(i) **1⇒2 Isochoric heating** Heat is added to the system at constant volume resulting in a pressure rise (Q_{in}) (fig 4a, stage 1-2 in fig 3).
(ii) **2⇒3 Isothermal expansion** Heat continues to be added to the system, the temperature however remains constant whilst the volume increases; work is extracted from the system (W_{out}) (fig 4b, stage 2-3 in fig 3).
(iii) **3⇒4 Isochoric cooling** Heat is removed from the system at constant volume whilst the pressure drops (Q_{out}) (fig 4c, stage 3-4 in fig 3).
(iv) **4⇒1 Isothermal compression** Heat is removed from the system whilst the temperature remains constant and the volume decreases (W_{in}) (fig 4d, stage 4-1 in fig 3).

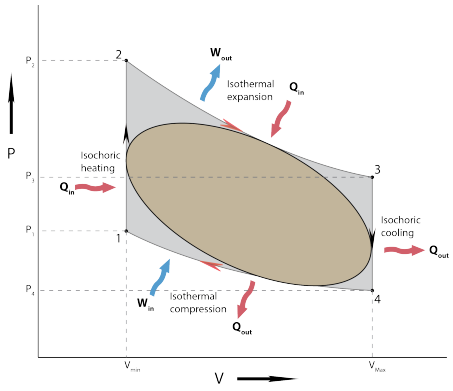

Fig. 3: Idealised Sterling cycle; pressure vs volume.

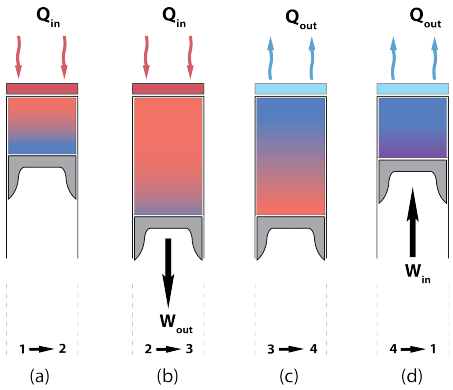

Fig. 4: Simple Stirling cycle schematic.

It can be seen from figure 4 that it is difficult to devise a practical way of introducing heat to the system and then remove it at the same point of application.

2.2 Improved Stirling Cycle

A more practical and efficient system was proposed by Rev. Robert Stirling, his 'improved ideal Stirling cycle' [50] is presented in figure 5 in which a porous displacer (or regenerator) is added to the system allowing heat to be introduced (Q_{in}) and rejected (Q_{out}) at opposite ends of the cylinder; in this way a temperature differential can be exploited successfully. The schematic in figure 5 effectively contains a regenerator (displacer) sandwiched between two heat exchangers one of which is its self, a moving piston. It can be seen that the system more closely resembles that of a thermoacoustic device; the motion of the piston approximating to an acoustic wave.

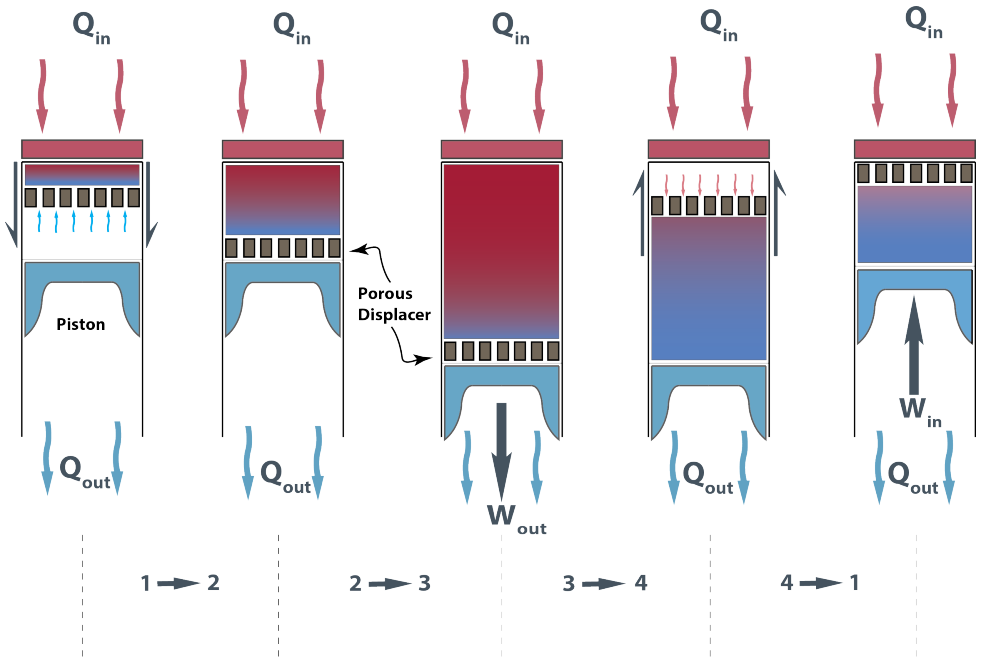

Fig. 5: Improved Stirling cycle - with displacer.

(i) **1⇒2 Isochoric heating** (at constant volume) The displacer moves (via mechanical linkage) from the hot end of the cylinder to the cold (piston) end. As it does so, the displacer gives up a proportion of its stored heat to pre-warm the working fluid as it flows through the regenerator and inhibits the transfer of heat from the hot end to the cold and is its self cooled.
(ii) **2⇒3 Isothermal expansion** Heat continues to be added to the system whilst the temperature remains constant, the volume increases and work is extracted.
(iii) **3⇒4 Isochoric cooling** The displacer is moved from the cold end to the hot end. Heat is removed from the working fluid as it is forced through the displacer.
(iv) **4⇒1 Isothermal compression** Heat continues to be removed from the system whilst the volume decreases and the transfer of heat into the system is again inhibited by the displacer as it is warmed.

The work per cycle is represented by the shaded area of the Stirling cycle in figure 3 and its approximate sinusoidal equivalent in the darker grey ellipse. Efficiency (as the ratio of net heat input and removed from the the system to the net work produced) is given by:

$$\eta = \frac{\text{work of compression - work of expansion}}{\text{heat removed} - \text{heat delivered}}$$

The ideal Stirling cycle (based on lossless, inviscid flow) has the maximum efficiency possible under the second law of thermodynamics, which is determined by the temperatures at which heat is accepted and rejected from the cycle, this is known as the Carnot limit defined by:

$$\eta_{carnot} = \frac{T_h - T_c}{T_h} \tag{1}$$

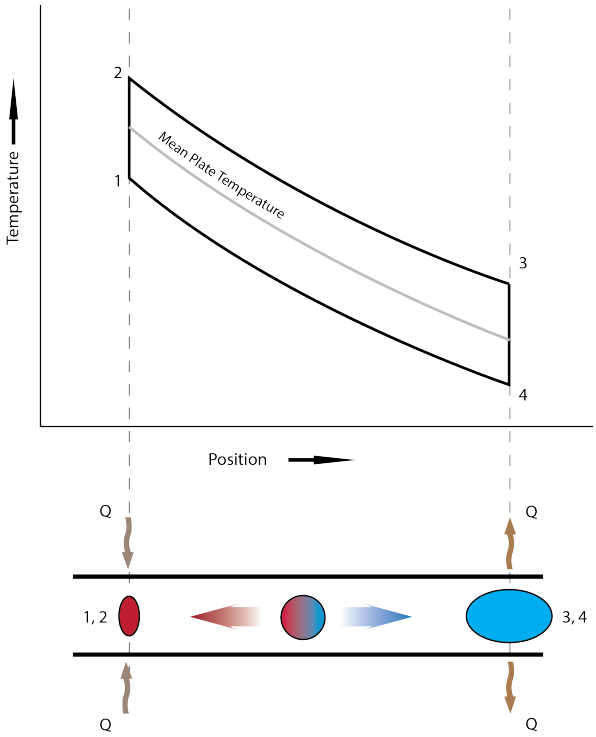

Fig. 6: Idealised thermo-acoustic cycle for an elemental gas parcel oscillating between a section of the plates of a regenerator with an applied temperature gradient - this process is repeated along the entire length of the plates, amplifying the acoustic wave.

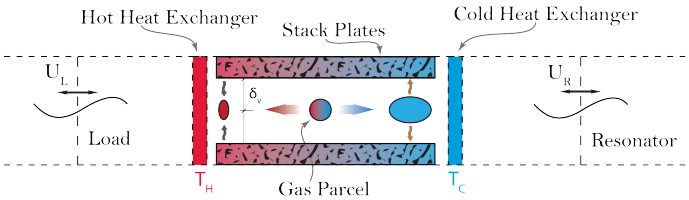

Fig. 7: Heat transfer between the plates in a thermoacoustic engine (TAE).

where T_h is the temperature of the hot reservoir and T_c is the temperature at which heat is rejected to the cold reservoir. It is the same cycle which occurs in the regenerator of a thermoacoustic engine (or pump) and since there are no moving parts in a thermo-acoustic device, efficiency losses relate to viscous losses, acoustic attenuation, 'dead' volume and inefficiencies in the heat exchangers. As an approximate guide, the efficiencies of the most advanced devices approach 40% of the Carnot limit [40], equivalent to a modern diesel engine.

3 Classification of Thermoacoustic devices

Thermoacoustic devices are classified as;

(i) **Refrigerator / Heat Pump** - Devices which utilise an acoustic pressure wave to generate a temperature differential across the stack.
(ii) **Engine / Prime-mover** - Devices which exploit a temperature differential across the stack to amplify an acoustic pressure wave.

The concept of the critical temperature gradient, described in more detail in section 5.4, underpins the classification of thermoacoustic devices. The closely stacked plates in a thermoacoustic device act as a temporary heat store, accepting and rejecting it at appropriate points in the acoustic cycle. In a thermoacoustic refrigerator (TAR), the heat of compression is rejected to the stack plate at the point of maximum compression and accepted from the plate at the point of maximum rarefaction building the temperature gradient which is then utilised through heat exchangers. In a thermoacoustic engine (TAE) the heat is added to the working gas (via the hot heat exchanger) at the point of maximum compression and removed (via the ambient heat exchanger) at the point of maximum rarefaction; amplifying the wave (see figure 7).

These devices can be further classified into;

(a) **Standing Wave Devices** - Those devices in which the geometry of the apparatus is designed to sustain a standing wave and benefit from a natural phasing between the velocity and pressure amplitudes which facilitates the thermoacoustic effect as set out in section 2.
(b) **Travelling Wave Devices** - Those devices in which the acoustic wave traverses the device in the direction of wave propagation, this means that the natural phasing is lost and has to be enforced through an acoustic network of inertances (analogous to the inertia or inductance of the gas) and compliances, described in more detail in section 6.2

4 Current activity in Thermoacoustics

The task of identifying groups currently engaged in research and development in thermoacoustics is not easy owing to issues of commercial sensitivity, the following is an attempt to summarise; apologies for any omissions.

According to Poese [41] in recent years a number of commercial companies have shown interest in the field and have been issued patents; IBM [20], Modine Manufacturing [3] (a heat exchanger manufacturer) and Praxair [44] (gas liquefaction) amongst others.

The Ford Motor Company has published its research and presented its findings to the Acoustical Society of America [31] but most other commercial organisations are less forthcoming.

'Ben and Jerry's' Ice-cream (Unilever) [53] in close affiliation with Pennsylvania State University have produced a working prototype for use in their 'in store' chiller cabinets. This has spawned a company called Thermoacoustics Corp $\sim$ 'Sounds-Cool' based at Pennsylvania State University. This work has also led to a collaboration with Volvo for recovery of waste heat in truck exhaust systems through Clean Power resources Ltd. [2].

A patent search reveals a number of companies and academic institutions around the world currently involved in thermoacoustics. It is thought that in the US only The Universities of Maryland, Mississippi, Utah, Pennsylvania State, the Los Alamos National Laboratory, the Naval Post-Graduate School and Purdue University have working thermoacoustic systems.

In Japan an association of around 100 researchers from industry and academia are working on thermoacoustic refrigeration and pulse tube cooling. Much of this work is based at Doshisha University.

The Honda Motor Co. Ltd. [5] has recently registered patents as has the Saudi 'King Abdul Aziz City for Science and Technology' [24], the Beijing Institute of Civil Engineering, Toyota Motor Corporation [4] and Hitachi Ltd. [18].

The Jawaharlal Nehru Centre for Advanced Scientific research in Bangalore, India has interests in thermoacoustics.

In Europe, the ASTER^{TM} [7] Thermoacoustic project now partnered with THATEA^{TM} in the Netherlands has published much of its work, has filed several patents and contributed greatly to the knowledge pool. The work of this group focuses on the recovery of low grade waste heat and on solar cooling. Pierens and Duthil [40] summarising the project claim an output of 600W from a temperature difference of 233K and at an efficiency approaching 40% of the Carnot limit.

The Institut de Physique Nucleaire d'Orsay in Paris [59] has a pilot project to produce a Cryogenic thermoacoustic cooler for the liquefaction of natural gas funded from multiple sources.

In the UK the Score-Stove(TM) project [1] at Nottingham University aims to produce an acoustically driven stove and refrigerator in association with energy company Alstom UK, 'Engineers Without Borders' are supporting the project through their work at Kathmandu University. The project also involves Universities of Manchester, Imperial College London and Queen Mary, University of London.

Thermoacoustics, primarily with reference to burner instability, is researched at Cambridge University.

Nouh et al. [34] based at the University of Maryland in the United States have recently published extensively on the use of thermaoacoustics and piezoelectric transducers as energy harvesting systems as set out in section 6.5.2.

Whist not an exhaustive list, the foregoing provides a feel for the current state of the art.

5 Critical performance parameters

The critical performance parameters associated with thermoacoustic devices are interdependent and often highly non-linear in nature. Whilst it is possible to evaluate each parameter independently to arrive at an ideal solution, the coupled non-linear effects of each parameter upon the others makes numerical modelling computationally expensive.

The key parameters influencing device performance are:

(i) plate spacing in the stack,
(ii) stack geometry,
(iii) critical temperature gradient,
(iv) working fluid properties,
(v) mean pressure - the fill pressure of the device,
(vi) drive ratio - pressure amplitude,
(vii) frequency.

5.1 Plate spacing

The correct spacing of the plates within a thermoacoustic stack is fundamental to the way in which these devices work. This spacing is a function of the viscous and thermal penetration depths of the working fluid (δ_ν and δ_κ respectively) and the ratio of the square of these two values which is the Prandtl number (described in greater detail in section 5.5.2) In a standing wave, the velocity and pressure are approximately

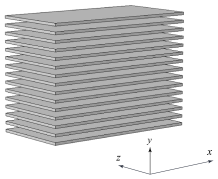

Fig. 8: Parallel plate stack

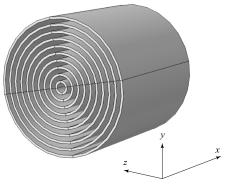

Fig. 9: Concentric stack

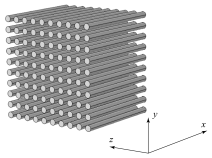

Fig. 10: Pin array stack

90 ° out of phase. Any element of working fluid greater than a thermal or viscous penetration depth from the surface of a plate in the stack will 'feel' no effect of the presence of that plate, i.e there will be no heat transfer and no viscous effect. The viscous and thermal penetration depths are a function of the angular velocity (ω) of the fluid and of the thermal properties of the fluid. A natural phasing is imposed upon the wave as a result of the no-slip boundary condition at the plate surface which facilitates the thermoacoustic effect; the compression and rarefaction of the gas in the acoustic wave is essentially adiabatic beyond a thermal penetration depth (δ_κ) but the same process is almost isothermal at the plate surface where the temperature of the gas is locked to that of the plate. This natural phasing is only present in standing wave devices, the plate spacing is typically a small multiple of penetration depths. A travelling wave device, in which the plate spacing is much closer (usually a fraction of a penetration depth) does not benefit from this natural phasing and consequently it must be imposed through an acoustic network which includes compliances and inertances. (see section 6.2 on page 17)

Tijani et al. [60] experimentally evaluated a range of plate spacings for a thermoacoustic stack for use in a standing wave device which supported the case for a plate spacing of $2.5\,\delta_\kappa$ for maximum cooling power; $4.0\,\delta_\kappa$ to attain the lowest temperature and $3.0\,\delta_\kappa$ for optimal overall performance.

The study used helium gas at a mean pressure of 10 bar at an operating frequency of 400Hz. The thermal penetration depth (δ_κ) was 0.1mm with a viscous penetration δ_ν depth of 0.08mm i.e. a Prandtl No. approaching unity. The pressure ratio, i.e. the ratio between the mean pressure and the maximum amplitude of the pressure wave, (defined further in section 5.7) was 1.4.

The thermal properties of the Mylar plate were; a thermal conductivity of 0.16 W/mK and a specific heat capacity (C_p) of approximately 1.24 kJ/kg K. The effect of frequency upon the heat transfer process with the given thermal properties is worthy of further investigation since the heat transfer process is heavily reliant upon the angular velocity of the wave and by implication, the contact time available for the heat transfer to occur.

Hariharan et al. [14] have investigated the effects of the stack length (in the direction of wave propagation x), its position in the resonator and the plate spacing. The critical temperature gradient and pressure amplitude were found to increase with an increase in resonator length for a given stack length (50mm). The resonant frequency was also found to increase with a decrease in resonator length as one would expect. A decrease in stack length also led to an increase in the resonant frequency. The experimental results were compared to the predicted values using DeltaE software and were found to be within 10% of the predicted values.

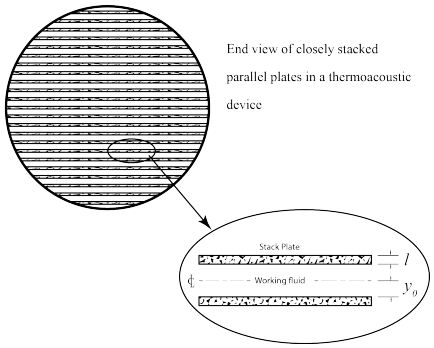

Fig. 11: Nomenclature used in plate spacing.

5.2 Plate thickness

Hariharan et al. [15] introduce the interesting concept of thermal penetration depth for the *solid* material from which the plates are fabricated given by:

$$\delta_s = \sqrt{\frac{2k_s}{\omega\,\rho_s\,C_{p,s}}}$$

Where k_s is the thermal conductivity of the solid used to fabricate the plates, ω is the angular frequency of the wave, ρ is the density of the solid and $C_{p,s}$ is the specific heat capacity of the solid.

Since the stack plates act as a temporary heat storage (for the duration of an acoustic cycle), it must have a specific heat capacity greater than that of the gas in immediate contact with it but must not conduct that heat axially along the stack thus permitting the leakage of heat down the temperature gradient. This has a bearing on the minimum thickness for the plates and, in turn, an influence upon the blockage ratio.

5.2.1 Blockage ratio and Hydraulic radius

Figure 11 shows a cross section of the stack and the nomenclature used. The dimensionless blockage ratio (ratio of open cross sectional area to stack plate cross section) for a parallel plate stack is given by;

$$B = \frac{y_0}{y_0 + l}$$

where y_0 is the half plate spacing and l is the plate thickness; it relates the cross sectional area of the stack available to the free passage of the acoustic wave.

Since optimising the blockage ratio and hydraulic radius is of prime importance the limiting design parameter is the thickness (and by implication the mechanical and thermal properties) of the plates themselves, the blockage ratio is a function of the plate thickness, spacing and the spacing of any interstitial supporting material.

The flexural rigidity of the material then becomes the limiting factor:

$$EI\frac{dy}{dx} = \int_0^x M(x)\,dx + C_1$$

Where E represents Young's modulus, I is the 2^{nd} moment of area of the cross section, M is the applied bending moment and C_1 is the constant of integration.

and since flexural rigidity is given by;

$$D = \frac{E\,l^3}{12(1-\nu^2)}$$

Where ν is the Poisons ratio of the material, and l is the thickness of the material.

it can be seen that the sensitivity of D is determined by the cubed term for thickness (l) in the numerator. A proportional increase in the modulus of the material is required to offset a small decrease in the value of the thickness and the second moment of area. This implies that the modulus of the material is critical in maintaining a low blockage ratio for the device.

Additional stiffness could also be attained by tensioning the material in a parallel plate stack, sufficient to raise the natural frequency of the plate above that of the driving frequency of the device. Although the harmonics and non linear effects would still need to be mitigated. (see future design considerations).

It is interesting to note that since the thermal capacity and conductivity of the material in the stack plates is also critical to the performance of the device it is important to give consideration to these design parameters when attempting to optimise the dimensions of the plates. Control over the thermal properties of the plates is a fundamental design requirement; an anisotropic distribution of thermal properties favouring conductivity in the y direction (from/to the working fluid) over the x direction (the direction of wave propagation and thermal gradient) would appear to offer the optimal design characteristic. These considerations are of even greater importance in the case of a regenerator (for use in a travelling wave device) in which the plate spacing is often only a fraction of a thermal or viscous penetration depth. The need to optimise the blockage ratio and hydraulic radius is, in this circumstance, paramount.

5.3 Stack geometry

Referring to figures 8, 9 and 10, the stack geometry is typically an arrangement of closely stacked parallel plates or approximation of an infinite parallel place by spirally coiling the material (modelled using concentric rings here) or as parallel pins. In each case the material from which the stack is fabricated acts as a temporary thermal store and the working gas must be within a specified hydraulic radius of the plates (r_h) as set out in section 5.2.1.

Petculescu and Wilen [39] assert that innovative stack geometries have the potential to increase the efficiency of thermoacoustic devices. Nessler and Keolian [32] calculated that Pin arrays (fig. 10) would offer enhanced efficiency and their calculations were later verified experimentally by Hayden and Swift [17]. Pursuant to this line of thinking it might well be that stacks which deviate from a uniform cross section might offer significant benefits; Rott et al. [48] have calculated the effect of a flared or conical shaped tube on the stability equation for a Sondhauss tube. Lightfoot [25] in his thesis also showed that it might be possible to increase the efficiency of a parallel plate stack by varying the plate spacing along the temperature gradient.

Zink et al. [70] have investigated a range of optimisation strategies for the thermoacoustic stack or regenerator as have Babaei and Siddiqui [8] who provide a flow chart approach for a new thermoacoustic design algorithm. The process begins with

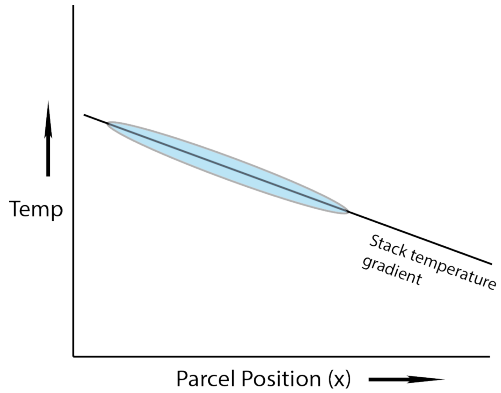

Fig. 12: Critical temperature gradient - the temperature a given parcel of gas matches the temperature of the stack plate.

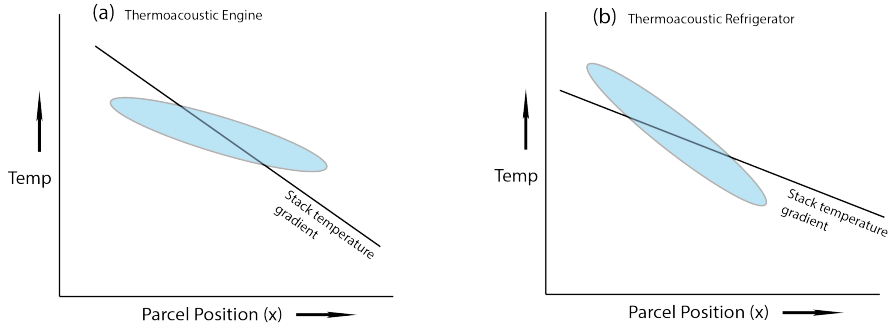

Fig. 13: 'Onset temperature gradient - leading either to amplification of the acoustic wave (a) or the pumping of heat up the temperature gradient (b).

the properties of the working gas and follows this through to the design of the stack geometry and ultimately energy balance equations which determine the efficiency of the component parts of the device. The authors claim that the procedure significantly reduces the technical challenges associated with designing thermoacoustic devices - compared to using DeltaE. the proposed design algorithm is designed to be used for thermoacoustically driven refrigerators (i.e. a prime mover generating a pressure wave and then using that pressure wave to pump heat).

5.4 Critical temperature gradient

The critical temperature gradient is the temperature gradient through the length of the stack plates in the direction of wave propagation which matches the temperature changes in the working fluid. Figure 12 shows the hysteresis loop undergone by the gas during its compression and rarefaction (as in figure 6); and the temperature gradient of the plate. It can be seen that under these conditions no acoustic work is done by the system and the temperature of the plate approaches that of the gas in contact with it at each point in the acoustic cycle

A more useful parameter is often referred to as the 'Onset temperature gradient' (see figure 13; the gradient at which acoustic work is done, either through amplifica-

tion of the acoustic wave as in (a) or by pumping heat up the temperature gradient as in (b).

This onset gradient has been determined both empirically and through a range of numerical studies, Tu et al. [62] for example, have derived a transfer-matrix for the acoustic attenuation which takes place at a range of temperature gradients and validated it. The process in the stack is assumed to be non-isothermal but the conductivity of the material through the length of the stack which has an influence upon acoustic attenuation, is not evaluated. Wu et al. [65] have applied a different approach by measuring the temperature gradient developed across the stack as cooling load in a thermoacoustic refrigerator. A range of parameters are evaluated including plate spacing, thickness, length and operating frequency.

Yu and Jaworski [68] have investigated low onset temperature devices and optimised the thermoacoustic stack for this particular parameter since it is of prime importance in energy harvesting situations where low grade waste heat is available.

5.5 Working fluid

The properties of the working fluid have a significant impact upon the performance and efficiency of thermoacoustic devices, the choices made with regard to the composition of the gas also have implications for the design options for such devices. Swift [58] uses dimensional analysis to illustrate that thermoacoustic power scales as $p_m aA$ and thus, for a given $|p_1|/p_m$ (drive ratio or the ratio of maximum pressure amplitude to mean pressure) high mean pressure and a high speed of sound yield the highest power for a given device as a function of volume. The speed of sound is highest in the lightest gasses ($H_2\,, He\,, Ne$). These gasses are particularly suited to low temperature (cryo-cooling) applications where heavier gasses either condense, freeze or have non-ideal behaviour.

The thermal conductivity of these light gasses is also high which leads to higher thermal penetration depths (δ_κ) and hydraulic radius allowing larger plate spacing. Opposing this, a high mean pressure reduces δ_κ and leads to closer plate spacing. Hariharan et al. [15] also states that the choice of working fluid influences the onset temperature gradient as a result of sound speed and high thermal conductivity which provides a greater power density owing to the larger thermal penetration depth. A range of gas (predominantly binary) mixtures have been used in order to optimise this critical performance parameter.

As an example of the use of an extremely low Prandtl number (the ratio of viscous diffusivity to thermal diffusivity - see section 5.5.2); Migliori and Swift [29] describe the construction of a thermoacoustic engine using liquid sodium as a working fluid. The authors suggest that the power density is comparable to that of a conventional heat engine but that the measured performance disagrees substantially with the numerical calculations based on Rott's thermoacoustic approximations which assume ideal behaviour. The author was unable to explain this behaviour at the time of publication.

Ho et al. [19] have postulated a design for a thermoacoustic refrigerator base upon a stress induced phase change in NiMnGa. The authors propose a suspension of NiMnGa nanoparticles which would have the potential to increase the heat capacity of the woking medium. An analogy is drawn between the gaseous-liquid phase transformation in a vapour compression refrigerator and the stress induced phase transformation in NiMnGa proposed by the authors. Acoustic pressure oscillations, whilst being insufficient to effect a phase change in a vapour compression cycle might however be used to effect a stress induced phase-change in a suitable material. In the

design proposed by Ho et al. [19], the acoustic pressure oscillations are provided by a lead zirconium titanate (PZT) piezoelectric transducer material.

Whist this theory presents opportunities for a rich vein of research, it should be noted that Spoor and Swift [54] of the Condensed Matter and Thermal Physics group at Los Alamos National Laboratory identified a previously unknown thermoacoustic phenomenon, whereby a mixture of helium and argon is separated as a result of (the authors postulate) the thermal diffusion gradient and viscous boundary layer effects acting upon the differing molecular masses of the component gasses. A mixture separation representing a 7% difference in the concentration of the two constituent gasses was observed. A mechanism is suggested and further research outlined. It is entirely possible that in seeding the working fluid with NiMnGA nanoparticles as suggested by Ho et al. [19], complex streaming and separation might occur leading to complex non-linear phenomenon. It is also possible that the same might apply to binary gas mixtures used to influence the Prandtl no. as outlined in section 5.5.2.

5.5.1 Properties of the working fluid

The choice of working gas must encompass:

(i) ratio of specific heat capacities,
(ii) thermal conductivity,
(iii) viscosity,
(iv) isothermal and Adiabatic Bulk modulus,
(v) density,
(vi) toxicity,
(vii) safety,
(viii) environmental impact.

5.5.2 Prandtl number

The dimensionless Prandtl number (p_r) provides the most convenient method of evaluating a fluid's thermal and viscous properties; it is the ratio of viscous diffusivity to thermal diffusivity and is given by:

$$P_r = \frac{\mu C_p}{\kappa}$$

Where μ is the dynamic viscosity, C_p is the specific heat capacity at constant pressure and κ is the thermal diffusivity. Campo et al. [10] Give a comprehensive overview of the impact of the Prandtl no. on the performance of a travelling wave thermoacoustic device - a very low Prandtl no. is preferred since this minimises the viscous losses and allows a larger hydraulic radius (plate spacing) as a consequence of the large thermal penetration depth.

The Prandtl no. for the mix is given by:

$$Pr_{mix} = \frac{\mu_{mix} C_{p,mix}}{\kappa_{mix}}$$

Campo et al. [10] also give detailed explanation of the use of the kinetic gas theory to calculate $P_{r,mix}$ for a range of gas mixtures with a Helium - Xenon mix of 0.975 mole fraction of Xenon giving a Prandtl number of just 0.12. Swift [58] points out that the addition of Xenon to the mix also lowers the speed of sound which in turn leads to a lower power per unit volume. A study on the way in which this coupling

can best be optimised forms an important part of the current research. An extreme example of a low Prandtl number is presented by Migliori and Swift [29] as outlined above in which liquid sodium with a P_r between 0.005 to 0.010 is used as a working fluid.

5.6 Mean pressure

Hariharan et al. [16] found that, for a twin thermoacoustic prime mover (TAPM) the onset temperature (the temperature gradient) at which the acoustic oscillations begin, increased with an increase in mean pressure. The critical temperature gradient is given by;

$$\nabla T_{critical} = \frac{\omega A \left|p_1\right|}{\rho_m \, c_{p,s} |U_1|}$$

where A is area, ρ_m is the mean density of the fluid, $C_{p,s}$ is the specific heat capacity of the plate, $|p_1|$ and $|U_1|$ are the 1^{st} order pressure and volumetric flow rates respectively.

The gradients sensitivity to changes in mean pressure can be clearly seen, since density is also a function of the mean pressure but the speed of sound is not and therefore the 1^{st} order volumetric flow rate $|U_1|$ is also unaffected.

Hariharan et al. [16] did however find that an increase in charge (mean) pressure leads to a significant increase in pressure amplitude. The results are within 10% of the predicted values from DeltAE and are in accordance with the findings of Swift [58] and Rott's thermoacoustic approximation.

5.7 Pressure amplitude or Drive ratio

Defined as the ratio of peak pressure amplitude of the acoustic wave to that of the mean (fill or charge) pressure in the device; The pressure amplitude attained from a thermoacoustic prime mover is a key performance parameter, as outlined above, the pressure amplitude is also a function of the mean pressure.

The drive ratio is defined as the pressure amplitude of the acoustic wave imposed by the piston of a thermoacoustic refrigerator (heat pump). A typical value used in an experimental set-up would be 1.4 (meaning that a 100kPa fill pressure would experience a high pressure amplitude of 140kPa and a low pressure amplitude of 60kPA).

5.8 Frequency

According to Swift [57] and Tijani et al. [61] the power density of a thermoacoustic device is a linear function of the acoustic resonance frequency; whilst δ_κ is inversely proportional to the square root of the frequency which requires a close plate spacing or hydraulic radius. In energy harvesting applications power density is a function of frequency, a high frequency being favoured which implies a close plate spacing. Linear alternators have been used to convert acoustic power to electrical however the inertia associated with such devices limits the practical operating frequency and several studies have been carried out using Piezoelectric aternators where the frequency at which these devices operate is more appropriate (300-700Hz); energy density being a function of frequency. The frequency at which a device operates is dictated largely by the geometry of the resonator and any Helmoltz volume (compliance). There are

examples of low frequency high amplitude devices, Liu et al. [26] have investigated the effects of frequency and stack position in thermoacoustic devices and their paper provides some useful insight. The lower frequency has implications for the thermal penetration depth of the working gas and of the material from which the stack is manufactured, as well as the size of the device since the natural frequency of the resonator will need to be matched to the operating frequency.

6 Analysis methodology

A range of analysis methodologies have been reviewed; Thermoacoustics present significant challenges owing to the complex multi-physical nature of the phenomenon. The process involves resolving compressible flow, acoustics, heat transfer, transient and non-linear behaviour; as a result it is often necessary to utilise a range of methodologies in order to arrive at a reliable result. Ultimately, data collected from experimental rigs is critical in validating any predictions.

6.1 DELTAE^{TM}

DELTAE (Design Environment for Low Amplitude Thermoacoustic Engines) was written by Ward and Swift [63] and is an established method of designing low amplitude devices. The user is taken though a simple process which permits sensible choices to be made with regard to the dimensions of the key components. A principle use of this software is in validating and benchmarking numerical analysis and empirical data; the majority of the current literature makes some comparison between the performance values predicted by DELTAE and those attained by experiment or numerical analysis. The software solves the 1 dimensional wave equation for an acoustic approximation in accordance with Rott et al. [48]. The software is being rapidly sidelined by modern multi-physics analysis packages but still has a roll to play in designing the acoustic network and predicting the acoustic behaviour of resonators etc..

6.2 Lumped parameter AC circuit analogy

As in many engineering disciplines it is convenient to draw analogies between acoustic networks and those of alternating current electrical networks; table 1 summarises the chief variables in this form of analysis and their counterparts in AC circuits.

Nouh et al. [35] describe the analysis of a thermoacoustic energy harvester. The performance of the device is modelled using electrical circuit analogy and using SPICE^{TM} (Simulation Programme with Integrated Circuit Emphasis) The results are compared with those produced by DeltaE software; the authors claim that the methodology enables both and steady state analysis. A detailed derivation of the input variables for the AC analysis and schematic representations are included. The analysis methodology is fully validated by the authors using an experimental rig. Poese [42] In his thesis also uses a 'Lumped Parameter' AC circuit analysis to explain the key processes in a thermoacoustic refrigerator.

Sun et al. [56] use an AC analogy to simulate the coupling between a linear alternator and a travelling wave thermoacoustic device. An experimental rig is used to validate the results which highlight the role of resonances in the device. The power developed is demonstrated to be proportional to the square of the acoustic amplitude as expected and predicted by established theory. A similar approach is taken by Jin et al. [22].

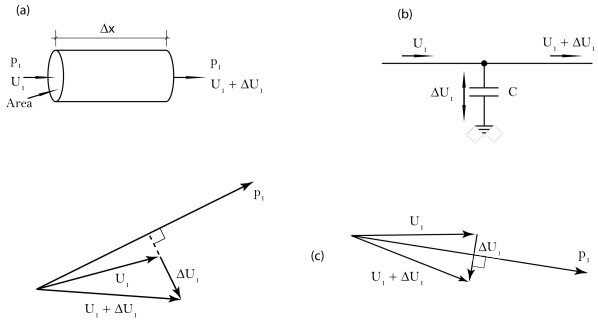

Fig. 14: AC Compliance/Capacitance (from Swift [58])

'SPICE^{TM}' is an open-source application written by the EECS Department of the University of California at Berkeley, USA. It is widely used to design electronic hardware but in this instance Nouh et al. [36] have successfully adapted its use for the analysis of thermoacoustic devices. The approach appears to have a good deal of potential for optimising devices prior to prototyping.

Riley [47] present a comprehensive analogue AC analysis of a thermoacoustic TAE. The role of each component group is explained and sample files provided. The phenomenon known as 'Squegging' ('an irregular oscillation characterised by short periods of oscillation punctuated by brief periods of quiescence' or unwanted Amplitude Modulation - AM) is described and simulated for the first time using an AC circuit analogy. The AC network is solved in TINA^{TM} (network analysis software), uses an empirically derived value for Carnot efficiency in the regenerator, and includes instrumentation components (velocity, pressure, power etc.) to interrogate the system parameters of the model.

Figure 14(a) shows a short channel in which the compressibility (compliance) of the gas is of interest; 14(b) gives a symbolic impedance diagram of the channel; 14(c) gives two example phasor diagrams; in each case the velocity U_1 is either augmented or diminished by the phase of the pressure vector in relation to the velocity.

Acoustic Parameter		AC Electrical Analogue	
Pressure	p_1	Voltage	V_1
Volume Flow rate	U_1	Current	I_1
Compliance	C	Capacitance	C
Inertance	L	Inductance	L
Resistance	R	Resistance	R
Acoustic power	$\dot{E}$	Electrical power	$\dot{W}$
Thermal Parameter		**AC Electrical Analogue**	
Temperature Gradient	T	Voltage	V
Heat Flux	$\dot{Q}$	Current	I
Thermal Mass	M	Capacitance	C
Thermal Resistance	h	Resistance	R

Table 1: Notation used in AC and Acoustic networks. Adapted from Swift [58] and [47]

Figure 15(a) shows a short channel in which the inertia of the gas is of interest; 15(b) gives a symbolic impedance diagram of the channel and 15(c) provides two possible phasor diagrams for the channel, the first in which the pressure amplitude is

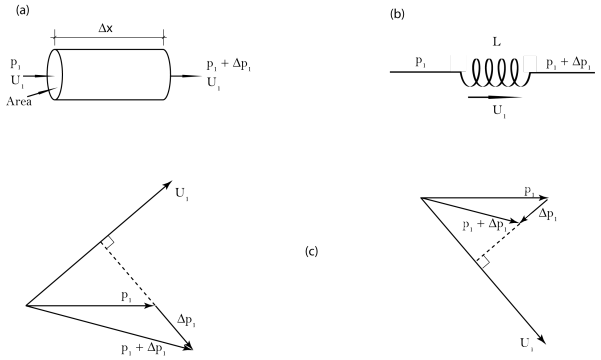

Fig. 15: AC Inertance / Inductance [58]

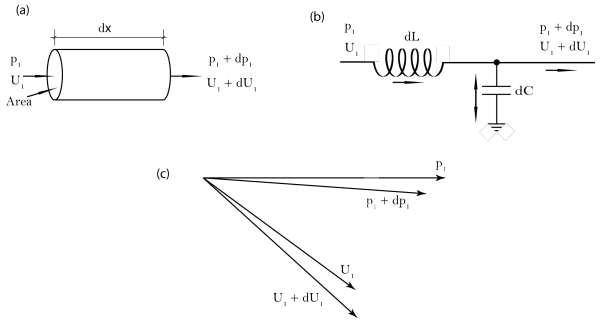

Fig. 16: AC Compliance and Inertance/ Capacitance and Inductance.[58]

augmented as a result of the inertia being 90° out of phase with the pressure wave; the other where the pressure amplitude is diminished as a result of the inertia being 90° out of phase in the opposite direction (imagine the inertia of the gas having been overcome and the gas already moving away from the pressure wave as it approaches).

Figure 16(a) shows a short channel in which both compressibility (compliance) and the inertia (inertance) are of interest; 16(b) shows the symbolic impedance diagram for the channel and 16(c) an example of a phasor diagram for the channel.

These AC representations are lossless, simplified by assuming inviscid flow. A true representation would include a viscous resistance with a dependency upon the square of the velocity. From this it can be seen that it is possible to represent the components in a program such as Matlab's 'Simulink' where a transfer function can be derived for each stage in the process.

6.3 Numerical (Multi-physics) analysis

The thermal and acoustic processes which take place in a thermoacoustic device are complex both in the literal sense and by mathematical definition. The coupling between the various types of physics involved is computationally expensive to model and whilst simplifications can be made, it is ultimately the geometrical constraints and the high aspect ratio of mesh elements and the disparity in the length scales within the device which lead to models typically taking days if not weeks to solve; even with access to high power computing services (HPC), as explored by Marx and Blanc-Benon [27]. For example, the viscous and thermal penetration depths of the

working fluid are often factions of a millimetre, giving plate spacing at a few hundred microns, but the wave length if these devices is often several orders of magnitude greater (approximately 1m). Resolving transient boundary layer effects whilst limiting node count in numerical models presents particular challenges.

Yu et al. [67] carried out a successful CFD analysis of a thermoacoustic engine running at 300Hz and was fully validated against an experimental rig. Non-linear effects were investigated and the acoustic flow vortices at either end of the stack of plates within the device. An upwind $2^n d$ order upwind spacial discretization was applied with time-step independence attained at 3.0×10^{-5} secs and mesh independence through refining the boundary layers in the stack and in the heat exchangers.

Yu et al. [66] used a CFD approach to study several important nonlinear phenomenon and processes of a large experimental thermoacoustic engine. The study successfully captures the onset temperature for the acoustic wave and the non-linear effect of mass flow through the device. Mass streaming is the subject of several studies notably that by So et al. [52] and by Kan et al. [23]. The vorticity and end effects of the stack are also successfully modelled by and the authors are sanguine that the approach remains valid for a range of thermoacoustic devices.

6.4 Dimensional analysis

As in other fields of engineering and physics, dimensional analysis is an important tool in the design and analysis of thermoacoustic devices. The work of Swift [58] sets out appropriate dimensionless groups used to simplify the analysis of thermoacoustic devices and provides examples.

A formal approach to similitude and dimensionless groups has been applied to Stirling Engines by Organ [38] and to thermo-acoustic engines and refrigerators by Olson and Swift [37]. For complete thermo-acoustic devices it may be convenient, they suggest, to use dimensionless groups from amongst the following (the subscript 0 being the ambient temperature or the ambient end of the stack):

$$\begin{gathered}
\frac{T(x,y,z,t)}{T_0},\ \frac{p(x,y,z,t)}{p_m},\ \frac{v(x,y,z,t)}{a_0},\ \frac{U(x,t)}{a_0 A_0},\ \frac{\dot{m}}{p_m/a_0} \\
\frac{\dot{Q}}{p_m a_0 A_0},\ \frac{\dot{W}}{p_m a_0 A_0},\ \frac{\dot{H}}{p_m a_0 A_0},\ \frac{\dot{E}_2}{p_m a_0 A_0} \\
\frac{x_j}{r_{h,0}},\ \frac{x_k}{\Delta_x},\ \frac{f\,\Delta_x}{a_0},\ \frac{\delta_{\kappa,0}}{r_{h,0}} \\
\gamma,\ \sigma_0,\ b_\mu,\ b_\kappa,\ k_{solid}/k_0
\end{gathered} \tag{2}$$

In which temperature (T) is non-dimensionalized by the ambient temperature; pressure (p) by the mean (fill) pressure (p_m) of the device; velocity (v) by the ambient speed of sound for the working gas (a_0); volumetric flow rate (U) by the product of ambient sound speed (a_0) and cross sectional area (A_0); mass flow rate ($\dot{m}$) by the ratio of mean pressure to sound speed. The rate of heat flux ($\dot{Q}$), Work ($\dot{W}$), total energy flux ($\dot{H}$), and second order acoustic power ($\dot{E}_2$) are non-dimensionalized by the product of mean pressure, ambient sound speed and cross sectional area. The hydraulic radius ($r_{0,0}$), speed of sound, and increments of x are used to non-dimensionalize thermal penetration depth ($\delta_{\kappa,0}$), the spacially averaged thermo-viscous function ($f\,\Delta_x$) and the geometric dimensions (x_j) and (x_k). The ratio of specific heat capacities

(γ), the Prandtl number (σ_0), thermal diffusivity of the solid (plates) and working gas(k_{solid}) and (k_0) respectively are used in accordance with standard fluid mechanics models.

Olson and Swift [37] give a comprehensive overview of the formal use of the Buckingham Pi theorem to derive appropriate dimensionless groups for the analysis of a thermoacoustic engine, similar to the one used by Swift [58]. The authors suggest that the approach is valid even for large pressure amplitudes and non-linear behaviour. Four specific worked examples are presented and equation 3 is applied in each case to ensure that the design parameters are met and retain similitude with previous experimental set-ups.

$$\begin{pmatrix} fL/a_{ref} \\ T(x,t)/T_{ref} \\ p(x,t)/p_m \\ v(x,t)/a_{ref} \\ \dot{W}/P_m a_{ref} A_{ref} \end{pmatrix} = g \begin{pmatrix} A_{ref}\, L_2, h_{ref}\, L, x_j\, L \\ \gamma, \sigma_{ref}, b_\mu, b_k \\ \breve{\epsilon}_{s,i},\ K_{ref} \\ \dot{Q}\,/P_m a_{ref} A_{ref}, \delta_\kappa/h_{ref} \end{pmatrix} \tag{3}$$

6.5 Energy conversion

In an energy harvesting context, the ability for a device to be able to take advantage of a small temperature difference is particularly important. The onset temperature difference is dictated by many interdependent factors as outlined earlier (see section 5.4). The mean (or fill) pressure for the device is particularly important. The best way to visualise this is to consider a gas at very low pressure (below atmospheric), the gas under these conditions is very compliant and a small temperature difference is capable of causing a large displacement. The converse is true of a working gas at very high pressure (200bar) as born out by the work of Hariharan et al. [16]. At the same time, a high mean pressure will yield a higher pressure amplitude for a given temperature difference. Converting the acoustic pressure wave into electrical energy, or making use of it in other ways, has been the focus of several studies over the last few years.

6.5.1 Linear Alternator

Several studies have focussed upon the use of linear alternators including Gonen and Grossman [12], Yu et al. [69] and Poese [43]. The limiting factor in each case is the energy density attainable (a function of frequency) as a result of the inertia introduced into the system as the coil is propelled backwards and forwards.

Gonen and Grossman [12] have also looked at the frictional losses in a linear alternator, an experimental validation rig was based upon a DeltaE model and the work provided a useful benchmark for the mechanical and dynamic characteristics of a linear alternator with appropriate operating conditions.

6.5.2 Piezoelectric transducers

The attraction of using Piezoelectric transducer materials is their ability to function at high frequencies and at very small strains with inherently low inertia built into the system.

Smoker et al. [51] have investigated the use of a piezoelectric membrane positioned at the hard end of the resonator of a standing wave device which produced an acoustic

wave from a solar heat source. The acoustic wave is self excited and its magnitude agrees well with the predictions of the DeltaE software. The membrane is a PZT5A (lead zirconium titanate) material mounted in an aluminium ring, the authors tuned its natural frequency to that of the resonator (approximately 338Hz) using weights at the centre of the membrane. The temperature at the hot end of the stack was 790K and at the cold end 304K, the power conversion being approximately 9.7% equating to 0.21mW/cm^2. A later study by Nouh et al. [33] included the addition of a mass and spring system termed a 'dynamic magnifier' by the authors which it is claimed contributes to an increased performance. The mass is acted upon by the acoustic wave which then transfers the stress to the piezoelectric membrane through a spring which effectively amplifies the strain values attained. The addition of a small amount added mass appears not to influence unduly the operating frequency of the device and the work is experimentally validated in a later paper by the same authors (Nouh et al. [34])

Jensen and Raspet [21] used two thermoacoustic devices, each placed at opposite ends of a resonator with a centrally placed piezoelectric membrane. Each device was carefully phased to push and pull the membrane at a high frequency (1.37kHz) and a mean pressure of 10 bar. The device attained approximately 10% of the Carnot limit.

7 Manufacturing details

7.1 Materials

The selection of materials for the fabrication of the key components centres upon their thermal and mechanical properties. The high mean pressures (in some cases up to 200bar) and cyclic, high frequency loadings required for efficient devices place particular demands upon the structural integrity of the resonator and associated acoustic phasing network; the need to minimise acoustic and thermal losses adds further complexity to the design and fabrication of both test rigs and prototypes.

As previously mentioned the thermal properties of the plates in the stack are of primary importance, introducing some level of anisotropy to these properties is important as shown by Maynard [28] in his design for an anisotropic stack and heat exchanger (ASHE) in which the stack plates are chemically etched to reduce heat transfer in the direction of acoustic wave propagation.

Grove [13] in his thesis showed that the lay-up and fibre orientation of carbon fibre reinforced resins could be used to influence their thermal properties and to introduce thermal anisotropy to a component. This may well have applications in the fabrication of key components in the field of thermoacoustics, assisting in the control of heat transfer, minimising thermal losses, controlling the stiffness of the walls of acoustic components etc..

Adeff et al. [6] have experimented with reticulated vitreous carbon (RVC), an open pore brittle foam, for use as thermoacoustic stacks and found that it's performance; whilst lower than a carefully constructed parallel plate stack, is, never the less, acceptable when one takes into account the significantly lower costs and reductions in complexity. The group is currently looking at ways of increasing the density of the RVC (decreasing pore size) for future test rigs.

7.2 Stack / regenerator

Tijani et al. [60] provides a description of a manufacturing method for a simple parallel plate stack with spacing between the Mylar plates being provided by monofilament

fishing line of various thicknesses (weights) allowing a range of plate spacing (from 0.15mm to 0.7mm) to be investigated experimentally. The method proposed is rather ad hoc involving drawing the monofilament line through a glue-filled syringe to precoat it, the line is then wound around a set of brass posts to position the line accurately above the Mylar film whilst another layer of film is added and the process begun anew. In this way a stack is built up measuring 85mm in the x direction, 50mm in the y and 45mm in depth z direction. A pin array stack was not attempted owing to the difficulty of fabricating such a component.

The study does not appear to include the influence of the dimensions of the stack in the x direction (direction of wave propagation) and since there exists the potential for coupling between this parameter and position of the stack within the device with respect to the phasing of the standing wave, it is felt that this offers potential for further study. It is worth noting that all the stack configurations used in these experiments used the same length and width of stack, but that the number of plates varied as a function of their spacing and therefore the surface area available for heat transfer varies with the plate spacing.

Swift [58] describes a method of fabricating a stack in which the plates are formed from a coil of stainless steel some 50 μm in thickness and separated from each successive turn by a sheet of copper 250 μm thick. In this way an approximation to an infinite parallel plate can be achieved. The ends of the coiled stack have a series of fine webs electron-beam welded to the stainless steel to act as permanent spacers. The copper is etched out using Nitric acid to leave an accurately manufactured stack with a blockage ratio approaching 0.83 (83% open space). This structure pre-stresses the material and has the potential to contribute to its stiffness and help to damp out vibratory behaviour of the foil. This is also investigated in section 7.2.1. It is also true to say however that the potential for distortion in-service is increased owing to the overall length of the material incorporated into the coil.

Stainless steel is a relatively poor conductor (14 - 16 W/m.K) but has a high coefficient of expansion (16 - 18×10^{-6} m/K) and as such, fabricating fine stainless steel structures, in which a temperature gradient is maintained, are liable to deformation, uneven spacing and poor thermoacoustic performance as a result. [58] gives an example of a flat plate stack which was fabricated by the author at Los Alamos National Laboratory (LANL) in which high temperatures were required for brazing which resulted in warping and deformation rendering the stack almost unusable.

The construction of stacks and regenerators needs to take into account the in-service conditions and mitigate appropriately against the effects of expansion and contraction at the design stage. A rigorous finite element analysis of the mechanical behaviour of these critical components does not appear in the literature; given the fine manufacturing tolerances required and the effects of a departure from the design ideal, it would seem sensible to consider such a comprehensive study as part of the design process. See section 7.2.1.

7.2.1 Finite element analysis of concentric stack geometry

A mechanical, finite element analysis (FEA) of possible stack geometries has been carried out by the authors with a view to understanding the behaviour of a range of plate materials and evaluating appropriate manufacturing techniques. Figure 17 shows the deformation as a result of applying a 300K temperature gradient through the length of a stainless steel stack similar to the one described by Swift [58]. A fixed constraint is applied to the webs at either end of the model in the radial direction. It can be seen that this results in an unacceptable level of deformation, in which the plates are subjected to warping as a result of thermal expansion. The deformation

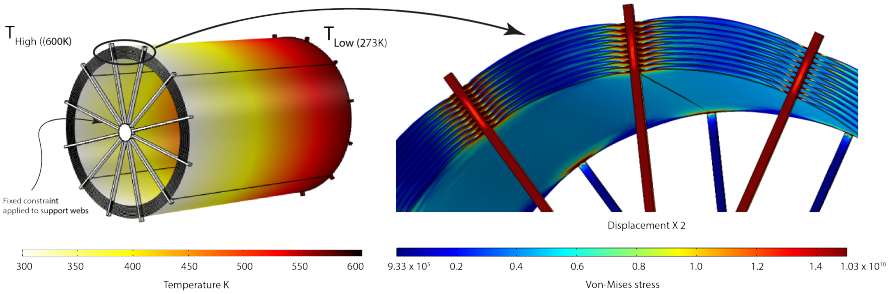

Fig. 17: Finite element analysis of a concentric stack

shown here is at 2 × true scale but it can be seen from figure **??** this equates to a displacement of 0.12mm which is approximately a thermal penetration depth in most devices. Parallel plates appear to provide a greater dimensional integrity and pin arrays appear to offer a significant advantage in this respect.

8 Conclusions and future prospects

Thermoacoustic energy harvesting appears to be based upon sound engineering principles and has much to offer and is;

(i) capable of utilising low grade wast heat,
(ii) able to operate using inert (non-toxic, environmentally friendly) working gasses,
(iii) capable of producing powerful acoustic pressure waves which can be converted into electrical energy,
(iv) able to act as the prime mover in thermoacoustic heat pumps, pulse tube cryocoolers and the liquefaction of gasses.

The following developments need to occur in order to allow the technology to reach its potential;

(i) A comprehensive, validated design methodology needs to be established.
(ii) The design of key components need to be refined and innovative solutions sought.
(iii) Appropriate materials for the fabrication of key components need to be identified or suitable composites defined and tested.
(iv) Heat exchanger designs capable of introducing and rejecting heat from the system without undue thermal or viscous attenuation of the acoustic wave will be required.
(v) Efficient mechanisms for converting acoustic energy to electrical energy will be required. Piezoelectric materials would seem to offer a good deal of potential in this area.

References

1. Score project, 2013. URL `http://www.score.uk.com/default.aspx`.
2. Clean Power Resources, 2015. URL `http://www.cleanpowerresources.com/thermoenergyconversion.php`.
3. Manufacturing Modine Ltd (1998). Thermo-acoustic system. *Patent No. WO1999020957 A1.*

4. Toyota Motor Co (2005). Thermoacoustic cooling device. *Patent No. JP2007315680*.
5. Honda Motor Co Ltd (2011). Thermoacoustic Engine. *Patent No. JP2011231941*.
6. Jay A Adeff, Thomas J Hofler, Anthony A Atchley, and William C Moss. Measurements with reticulated vitreous carbon stacks in thermoacoustic prime movers and refrigerators a). 104(1):32–38, 2014.
7. ASTER. ASTER - Thermoacoustics, 2015. URL `http://www.aster-thermoacoustics.com/`.
8. Hadi Babaei and Kamran Siddiqui. Design and optimization of thermoacoustic devices. *Energy Conversion and Management*, 49(12):3585–3598, December 2008.
9. G Bisio and G Rubatto. Sondhauss and Rijke oscillations, thermodynamic analysis, possible applications and analogies. *Energy*, 24(2):117–131, 1999.
10. Antonio Campo, Mohammad M. Papari, and Eiyad Abu-Nada. Estimation of the minimum Prandtl number for binary gas mixtures formed with light helium and certain heavier gases: Application to thermoacoustic refrigerators. *Applied Thermal Engineering*, 31(16):3142–3146, November 2011.
11. K T Feldman, H Hirsch, and R L Carier. Experiments on the Sondhauss Thermoacoustical Phenomenon. *The Journal of the Acoustical Society of America*, 39 (6):1236, 1966.
12. Eran Gonen and Gershon Grossman. Effect of variable mechanical resistance on electrodynamic alternator efficiency. *Energy Conversion and Management*, 88: 894–906, December 2014.
13. Stephen Michael Grove. Anisotropy of heat conduction in fibre-reinforced composites. *University of Plymouth*, 1985.
14. N. M. Hariharan, P. Sivashanmugam, and S. Kasthurirengan. Studies on Performance of Thermoacoustic Prime Mover. *Experimental Heat Transfer*, 28(3): 267–281, August 2014.
15. N.M. Hariharan, P. Sivashanmugam, and S. Kasthurirengan. Influence of stack geometry and resonator length on the performance of thermoacoustic engine. *Applied Acoustics*, 73(10):1052–1058, October 2012.
16. N.M. Hariharan, P. Sivashanmugam, and S. Kasthurirengan. Influence of operational and geometrical parameters on the performance of twin thermoacoustic prime mover. *International Journal of Heat and Mass Transfer*, 64:1183–1188, September 2013.
17. M E Hayden and G W Swift. Thermoacoustic relaxation in a pin-array stack. *The Journal of the Acoustical Society of America*, 102(November 1997):2714–2722, 1997.
18. Hitachi Ltd. (2003). Thermoacoustic heat pump / water heater. *Patent No. JP2005188846*.
19. Ken K. Ho, Eric Gans, Daniel D. Shin, and Gregory P. Carman. Stress Induced Phase Changing Material for Thermoacoustic Refrigeration. *Integrated Ferroelectrics*, 101(1):89–100, December 2008.
20. IBM (2012). Implementing Microscale Thermoacoustic Heat and Power Control for Processors and 3D Chipstacks. *Patent No. US20140083094*.
21. Carl Jensen and Richard Raspet. Thermoacoustic power conversion using a piezoelectric transducer. *The Journal of the Acoustical Society of America*, 128(1): 98–103, July 2010.
22. T Jin, B S Zhang, X M Zhong, and G B Chen. Preliminary Study on Circuit Simulation of Thermo Acoustic Engines. In *AIP*, volume 1103, pages 1–7, 2014.
23. Xuxian Kan, Feng Wu, Lingen Chen, Fengrui Sun, and Fangzhong Guo. Exergy efficiency optimization of a thermoacoustic engine with a complex heat transfer exponent. *International Journal of Sustainable Energy*, 29(4):220–232, December 2010.

24. King Abdul Aziz City for Science and Technology (2010). Standing Wave thermoacoustic / piezoelectric refrigerator. *Patent No. US2011252812*.
25. Jay A Lightfoot. *National Center for Physical Acoustics*. PhD thesis, University of Mississippi, 1997.
26. Yicai Liu, Tianlong Xin, Qian Huang, Xiangnan Shi, Siming Chen, and Lixin Chen. Coincident effect characteristic in a thermoacoustic regenerator. *Energy Conversion and Management*, 52(1):664–667, 2011.
27. David Marx and Philippe Blanc-Benon. Computation of the mean velocity field above a stack plate in a thermoacoustic refrigerator. *Comptes Rendus - Mecanique*, 332:867–874, 2004.
28. Julian D Maynard. Anisotropic heat exchanger and stack. Technical Report 0704, Penn State University, 2002.
29. A. Migliori and G. W. Swift. Liquid-sodium thermoacoustic engine. *Applied Physics Letters*, 53(5):355, 1988.
30. M P Mortell. Resonant thermal-acoustic oscillations. *International Journal of Engineering Science*, 9(1):175–192, 1971.
31. George Mozurkewich. A model for transverse heat transfer in thermoacoustic devices. In *December conference 1996*. The Acoustical Society of America.
32. F Scott Nessler and Robert M Keolian. *Comparison of a pin stack to a conventional stack in a thermoacoustic prime mover*. PhD thesis, 1995.
33. M. Nouh, O. Aldraihem, and A. Baz. Energy Harvesting of Thermoacoustic-Piezo Systems With a Dynamic Magnifier. *Journal of Vibration and Acoustics*, 134(6): 061015, October 2012.
34. M. Nouh, O. Aldraihem, and A. Baz. Optimum design of thermoacoustic-piezoelectric systems with dynamic magnifiers. *Engineering Optimization*, 46 (4):543–561, May 2013.
35. M. Nouh, O. Aldraihem, and A. Baz. Onset of Oscillations in Traveling Wave Thermo-Acoustic-Piezo-electric Harvesters Using Circuit Analogy and SPICE Modeling. *Journal of Dynamic Systems, Measurement, and Control*, 136(6): 061005, August 2014.
36. Mostafa Nouh, Osama Aldraihem, and Amr Baz. Transient characteristics and stability analysis of standing wave thermoacoustic-piezoelectric harvesters. *The Journal of the Acoustical Society of America*, 135(2):669–78, February 2014.
37. J R Olson and G W Swift. Similitude in thermoacoustics. *The Journal of the Acoustical Society of America*, 95(3):1405, 1994.
38. Allan J Organ. *The regenerator and the Stirling engine*. Mechanical Engineering Publications, London, 1997.
39. G Petculescu and L A Wilen. Thermoacoustics in a single pore with an applied temperature gradient. *The Journal of the Acoustical Society of America*, 106(May 1999):688–694, 2014.
40. M Pierens and P Duthil. Experimental characterization of a thermoacoustic travelling-wave refrigerator. 5(6):532–536, 2011. ISSN 2010376X.
41. Matthew E. Poese. Penn State University -Thermoacoustic refrigeration. URL `http://www.acs.psu.edu/thermoacoustics/refrigeration/faqs.htm`.
42. Matthew E. Poese. *An Evolution of Compact Thermoacoustic Refrigerator Design*. PhD thesis, Pennsylvania State University, 2004.
43. Matthew E Poese. Handbook of Climate Change Mitigation. Technical report, New York, NY, 2012.
44. Praxair (2002). Thermoacoustic cogeneration system. *United States Patent 6604364*.
45. B.J.W.S. Rayleigh. *The theory of sound*, volume 2. Macmillan, 1896.
46. P L Rijke. Notice of a new method of causing a vibration of the air contained in a tube open at both ends. *The London, Edinburgh, and Dublin Philosophical*

Magazine and Journal of Science LXXI, 17(116):419–422, 1859.
47. Paul H. Riley. Towards a Transient Simulation of Thermo-Acoustic Engines Using an Electrical Analogy. *Procedia Engineering*, 56(0):821–828, 2013.
48. By Nikolaus Rott, Gerassimos Zouzoulas, and Swiss Federal. Thermally Driven Acoustic Oscillations , Part IV : Tubes with Variable Cross-section. *The Journal of applied maths and Physiscs*, 27:197–224, 1976.
49. N Rott. Thermally driven acoustic ocillations. *Angew, Math, Phys.*,, 1(26):43–49, 1969.
50. Robert Sier. *Rev. Robert Stirling, DD: A Biography of the Inventor of the Heat Economiser & Stirling Cycle Engine*. LA Mair, 1995.
51. J. Smoker, M. Nouh, O. Aldraihem, and A. Baz. Energy harvesting from a standing wave thermoacoustic-piezoelectric resonator. *Journal of Applied Physics*, 111(10):104901, 2012.
52. J. H. So, G. W. Swift, and S. Backhaus. An internal streaming instability in regenerators. *The Journal of the Acoustical Society of America*, 120(4):1898, 2006.
53. Sounds-Cool. The Ben & Jerry ' s Project, 2005. URL `http://www.acs.psu.edu/thermoacoustics/refrigeration/benandjerrys.htm`.
54. P. Spoor and G. Swift. Thermoacoustic Separation of a He-Ar Mixture. *Physical Review Letters*, 85(8):1646–1649, 2000.
55. E M Stern and B Schlick-Nolte. *Early glass of the ancient world: 1600 BC-AD 50: Ernesto Wolf collection*. Verlag Gerd Hatje, Stockholm, 1994.
56. D.M. Sun, K. Wang, X.J. Zhang, Y.N. Guo, Y. Xu, and L.M. Qiu. A traveling-wave thermoacoustic electric generator with a variable electric R-C load. *Applied Energy*, 106:377–382, June 2013.
57. G W Swift. Thermoacoustic engines. *The Journal of applied maths and Physiscs*, 84(4):1145–1180, 1988.
58. Gregory W Swift. Thermoacoustics: A unifying perspective for some engines and refrigerators. *The Journal of the Acoustical Society of America*, 2003.
59. Jean-pierre Thermeau. "Thermoacoustics Is Going To Make a Lot of Nnnnnnnois". Technical report, Institut de Physique Nucléaire dOrsay, 2009.
60. M. E. H. Tijani, J. C. H. Zeegers, and a. T. a. M. de Waele. The optimal stack spacing for thermoacoustic refrigeration. *The Journal of the Acoustical Society of America*, 112(1):128, 2002.
61. M E H Tijani, J C H Zeegers, and ATAM De Waele. Design of thermoacoustic refrigerators. *Cryogenics*, 42(1):49–57, 2002.
62. Qiu Tu, Chih Wu, Qing Li, Feng Wu, and Fangzhong Guo. Influence of temperature gradient on acoustic characteristic parameters of stack in TAE. *International Journal of Engineering Science*, 41(12):1337–1349, July 2003.
63. Bill Ward and Gw Swift. Design Environment for Low-Amplitude ThermoAcoustic Engines (DeltaE) Tutorial and Users Guide (Version 5.1). *Los Alamos NationalLaboratory (June 2001)*, 2001.
64. John Wheatley, T Hofler, G W Swift, and A Migliori. An intrinsically irreversible thermoacoustic heat engine. 74(1):153–170, 2015.
65. Feng Wu, Lingen Chen, Anqing Shu, Xuxian Kan, Kun Wu, and Zhichun Yang. Constructal design of stack filled with parallel plates in standing-wave thermoacoustic cooler. *Cryogenics*, 49(3-4):107–111, March 2009.
66. G Y Yu, E C Luo, W Dai, and J Y Hu. Study of nonlinear processes of a large experimental thermoacoustic-Stirling heat engine by using computational fluid dynamics. *Journal of Applied Physics*, 102(7):74901, 2007.
67. Guoyao Yu, W. Dai, and Ercang Luo. CFD simulation of a 300 Hz thermoacoustic standing wave engine. *Cryogenics*, 50(9):615–622, 2010.

68. Z Yu and a J Jaworski. Optimization of thermoacoustic stacks for low onset temperature engines. In *Proceedings of the Institution of Mechanical Engineers, Part A: Journal of Power and Energy*, volume 224, pages 329–337, January 2010.
69. Zhibin Yu, Artur J. Jaworski, and Scott Backhaus. Travelling-wave thermoacoustic electricity generator using an ultra-compliant alternator for utilization of low-grade thermal energy. *Applied Energy*, 99:135–145, November 2012.
70. Florian Zink, Hamish Waterer, Rosalind Archer, and Laura Schaefer. Geometric optimization of a thermoacoustic regenerator. *International Journal of Thermal Sciences*, 48(12):2309–2322, December 2009.